Epilepsy Research (2009) **87**, 160—168

journal homepage: www.elsevier.com/locate/epilepsyres

EEG—fMRI study on the interictal and ictal generalized spike-wave discharges in patients with childhood absence epilepsy

Qifu Li[a,b], Cheng Luo[d], Tianhua Yang[a], Zhiping Yao[a], Li He[a], Ling Liu[a], Hongru Xu[a], Qiyong Gong[c], Dezhong Yao[d], Dong Zhou[a,*]

[a] *Department of Neurology, West China Hospital of Sichuan University, Chengdu 610041, Sichuan Province, PR China*
[b] *Department of Neurology, the Affiliated Hospital of Hainan Medical College, Haikou 570102, Hainan Province, PR China*
[c] *Huaxi MR Research Center (HMRRC), Department of Radiology, West China Hospital of Sichuan University, Chengdu 610041, Sichuan Province, PR China*
[d] *School of Life Science and Technology, University of Electronic Science and Technology of China, Chengdu 610054, Sichuan Province, PR China*

Received 11 March 2009; received in revised form 14 August 2009; accepted 22 August 2009

KEYWORDS
EEG—fMRI;
Absence epilepsy;
Ictal epileptic discharges;
Interictal epileptic discharges;
Basal ganglia—thalamocortical loops

Summary
Background: Absence epilepsy is characterized clinically by the impairment of consciousness and 3 Hz generalized spike-wave discharges (GSWDs) on EEG. Clinical absence can be observed with ictal GSWDs, but interictal GSWD bursts are usually clinically silent. Simultaneous EEG and blood-oxygen-level-dependent (BOLD) functional MRI (EEG—fMRI) has been successfully used to link the changes in regional neuronal activity to the occurrence of GSWDs.
Methods: We used EEG—fMRI to investigate and compare the BOLD signal changes during interictal and ictal GSWDs in patients with childhood absence epilepsy (CAE).
Results: Fifteen drug-naïve children with newly diagnosed CAE were studied using continuous EEG—fMRI. BOLD signal changes associated with interictal (nine sessions with six patients) and ictal (eight sessions with six patients) GSWDs were analyzed at the individual and group levels. GSWDs were associated with widespread and symmetrical deactivation in the cortex and caudate nucleus with a frontal maximum, and predominant activation in the thalamus bilaterally during ictal GSWDs and in the cortex during interictal GSWDs. The BOLD response was characterized by a higher statistical significance and a more widespread extent at the time of the ictal GSWDs as compared to the time of interictal GSWDs.
Conclusions: Both interictal and ictal GSWDs in patients with CAE are associated with BOLD signal changes in the basal ganglia—thalamocortical loop. Ictal GSWDs showing predominant

* Corresponding author.
E-mail address: zhoudong66@yahoo.cn (D. Zhou).

0920-1211/$ — see front matter
doi:10.1016/j.eplepsyres.2009.08.018

thalamic activation and widespread cortical deactivation might cause a complete suspension of the normal brain's default state and manifest clinically as abrupt loss of consciousness (absence seizures).

Introduction

An absence seizure is characterized clinically by the impairment of consciousness and 3 Hz generalized spike-wave discharges (GSWDs) on EEG (CCTILAE, 1981). With ictal 3-Hz GSWDs (duration often >4 s), abrupt and severe impairment of consciousness can be observed clinically, but GSWD bursts lasting <4 s (interictal GSWDs) are usually clinically silent (Van Luijtelaar et al., 1991). The underlying mechanisms for absence seizure have not yet been described. Furthermore, how GSWDs are generated and how these discharges relate to consciousness are still not fully understood (Hanneke et al., 2005). Recently, the possibility of combining EEG recording with functional MRI (EEG—fMRI) scanning provided the opportunity to reveal the brain regions showing blood-oxygen-level-dependent (BOLD) signal changes in response to the epileptic discharges seen on EEG (Stern, 2006; Gotman, 2008). This multimodal mapping technique has been used successfully to identify the regions that may be involved in focal epileptic disorders and idiopathic generalized epilepsy (IGE) (Laufs and Duncan, 2007). Although studies on clinical ictal activity are more important in discovering the mechanisms of this paroxysmal disease (Tyvaert et al., 2008), almost all present EEG—fMRI studies deal with interictal epileptic activity rather than seizures. It is difficult to predict seizure occurrence due to the short time of recording and the artifacts generated by movements (Laufs and Duncan, 2007). For absence epilepsy, two studies (Salek-Haddadi et al., 2003; Moeller et al., 2008a) involving a total of seven patients reported on the BOLD response to ictal GSWDs, and four studies (Aghakhani et al., 2004; Labate et al., 2005; Laufs et al., 2006; Hamandi et al., 2006) involving a total of 25 patients reported on the BOLD response to interictal GSWDs. Most previous studies demonstrated a thalamic increase in the regional BOLD signal along with a regional decrease in the cortex during GSWDs, but different regions of BOLD signal changes were also shown to vary from one study to another. The involved patients in previous studies were often limited, that is, there was only one patient in three studies (Salek-Haddadi et al., 2003; Labate et al., 2005; Laufs et al., 2006), or there were some confounding factors such as age, medication, and disease duration (Aghakhani et al., 2004; Hamandi et al., 2006). Moreover, there has been no study that focused on the different patterns of the BOLD signal in ictal and interictal GSWDs, although there is evidently a different clinical manifestation.

We investigated a homogeneous group of newly diagnosed and untreated children with CAE in order to assess the consistency and temporal pattern of network modulation as associated with ictal and interictal GSWDs, and furthermore, to compare the difference in BOLD signal changes between the interictal and ictal GSWDs.

Materials and methods

Subjects

This study was prospective and was performed at the epilepsy center of the West China Hospital of Sichuan University from July 2007 to August 2008. The study was approved by the Ethics Committee of the West China Hospital. We ensured that the patients and their families were informed about all research procedures and that they provided their consent before the experiment. Our study was performed according to the standards set by the Declaration of Helsinki. The diagnosis was made according to the ILAE 2001 classification scheme (Engel and ILAE, 2001). Patients who had CAE with frequent and stereotypical ictal and interictal GSWDs during a 24-h video EEG monitoring and no structural abnormalities on routine cranial CT and MRI were recruited. Patients who would not cooperate or had taken AEDs were excluded. Fifteen patients, seven males and eight females, aged 5—14 years (mean, 9.3) with an onset age of 4—9 years (mean 5.9), and who were diagnosed with childhood absence epilepsy, were recruited. The clinical details of the patients are shown in Table 1.

EEG acquisition

Electroencephalography was performed by using a 10/20 system with 34 Ag/AgCl electrodes soldered to 12 kΩ current-limiting impedance attached to the scalp with a conductive cream. The EEG device was a Mizar 40 amplifier (EBNeuro, Florence, Italy) with 32 channels adapted for MR. The sampling rate was set at 4 kHz, which allows a suitable time resolution for picking up the switching effect of the readout gradient in the high slew rate condition; the EEG dynamic range was kept at ±65.5 mV to prevent the MRI artifact from saturating the EEG/ECG. The EEG amplifier inside a shielded box was used to collect the signal and perform A/D conversion. The shielded amplifier was connected via a fiber optic cable to the recording monitor located outside the scanner room. The MR artifact could be filtered out online with the BE-MRI Tool box software (Galileo New Technology, Florence, Italy) (Garreffa et al., 2003). The ballistocardiographic effect was minimized through a careful arrangement of the EEG cables and an elastic cap. fMRI data were excluded if no GSWDs were found in real-time and offline filtered EEG in one session of a particular run.

The ictal GSWDs indicated that clinical absence was observed when the GSWDs burst on EEG. To confirm the absence onset during the scanning, the parents of the patients stayed in the MR scanner suite during the fMRI examination. When GSWDs occurred in the online filtered EEG, the parents were asked to monitor their children for any clinical signs of absences such as staring, eye deviation, and eyelid myoclonia. Therefore, the ictal GSWDs inside the scanner were defined strictly according to the following factors: (1) the GSWDs were similar to those recorded outside the scanner during typical absence seizures presented with a longer duration (>4 s) (Van Luijtelaar et al., 1991), and (2) the parents of the patients observed the clinical absence when the GSWD burst occurred. GSWD timing and duration were marked independently by two skilled electroencephalographers, and disagreements about the markers were resolved by discussion.

Table 1 Patient sex, age at seizure onset, seizure frequency, history and family history, and frequency of GSWDs.

ID no.	Sex	Age (years)	Seizure onset age (years)	Seizure frequency (times/day)	History/family history	Frequency of GSWDs (Hz)
1	M	5	4	40—50	—	3
2	F	5	4	10	—	3
3	F	9	6	20—30	—	3
4	F	7	6	Several	—	3—3.5
5	F	8	6	20—30	—	3
6	M	10	5	2—3	—	3—3.5
7	M	14	9	7—8	—	3—4
8	M	14	4	Several	—	3
9	F	5	4	10	—	3
10	M	12	7	2—3	Mother had GTCS	3—4
11	F	9	6	20—30	—	3
12	F	9	7	Several	—	3—4
13	M	7	4	20	Hypoxia history at birth	2.5—3.5
14	M	12	9	2—3	—	3.5
15	F	9	7	2—3	—	2.5—4

GTCS: generalized tonic-clonic seizures.

fMRI acquisition

A 3.0 T GE MRI scanner (EXCITE, Milwaukee, WI, USA) was used to acquire BOLD-sensitive echo-planar images (EPI) with continuous, simultaneous EEG. Foam padding was used to help secure the EEG leads, minimize motion, and improve patient comfort. The patients were packed with cotton in their ears, and they were asked to lie down and rest with their eyes closed. The imaging parameters of the gradient echo EPI sequences were as follows: 30 slices/volume, 200 volumes, TR = 2000 ms, TE = 30 ms, FOV = 24 cm × 24 cm, matrix = 64 × 64, in-plane resolution = 3.75 mm × 3.75 mm, and flip angle = 90°. The structural image was also acquired during the interval between the first and second run (TR = 8.5 ms, TE = 3.4 ms, field of view [FOV] = 24 cm × 24 cm, flip angle = 12°, matrix = 512 × 512, and 156 slices). The BOLD changes in fMRI data were collected in successive sessions of 6 min 40 s; additional sessions of scanning were required if a patient had no spikes recorded on real-time EEG in one session.

fMRI analysis

Functional MRI data were initially preprocessed according to the following four steps: (1) SPM2 software [www.fil.ion.ucl.ac.uk/spm] (Friston et al., 1994, 1995) was used to make a 3D rigid-body registration, spatial transformation, and realignment for the correction of head motion; (2) only signals in the brain to increase analysis efficiency were processed; voxels with values lower than a certain threshold (empirically to be 1/10 of the highest intensity in the input image) were regarded as background; (3) a spatial smoothing filter was employed for each brain 3D volume by convolution with an isotropic Gaussian kernel (FWHM = 6 mm for our data) to increase the MR signal-to-noise-ratio; and (4) a high-pass filter with a cut-off of 128 s was used to remove low-frequency noise and to reduce the effect of scanner instability and/or of a gross physiological change in the patients.

According to the EEG, the time point at which the interictal or ictal GSWDs were recorded was when the first spike-time signal was acquired. Then the canonical hemodynamic response function (HRF) was modeled by two gamma-variant functions (Friston et al., 1998) convolved with the spike-time signal. Finally, the canonical HRF was specified as an interested regressor in the SPM design matrix. The other six non-interested regressors were derived from the six parameters that were obtained by rigid-body correction of head motion. The special activated areas were calculated using statistical t tests with five contiguous voxels above a t value of 3.14 (uncorrected). In order to determine the relationship between subjects (second level), contrast images were created for each patient and were entered separately into voxelwise one-sample t tests, implementing a random effects analysis for each group. The cluster showing an uncorrected $P < 0.001$ and $|T| > 5.21$ (d.f. = 7) and $|T| > 4.79$ (d.f. = 8) for its spatial extent was considered significant.

Results

Three patients were excluded from further analysis, two due to lack of GSWDs (patients 9 and 14) and one (patient 15) due to excessive head motion (more than 1 mm and 1°). Eighteen sessions of EEG—fMRI scanning in 12 patients were carried out. In 10 sessions in 7 patients, interictal GSWDs were identified, and in the other 8 sessions, ictal GSWDs were produced in 6 patients who presented with repetitive absence seizure before and after fMRI scanning (Fig. 1). The number of interictal GSWD epochs ranged from 3 to 14 (median, 7), and the duration of an epoch ranged from 0.5 to 3.8 s. The number of ictal GSWDs epochs ranged from 1 to 11 (median, 2), and the duration ranged from 8 to 35 s (details in Table 2). Notably, there were two sessions in which BOLD changes in response to both interictal and ictal GSWDs were obtained in two successive EEG—fMRI scannings of one patient (Patient 5).

Individual analysis

All patients but one (patient 6, with interictal GSWDs) showed BOLD signal changes in response to GSWDs. These BOLD signal changes were mostly bilateral and symmetrical, and they involved the cortical and subcortical structures. A positive BOLD signal (activation) was recorded in the cortex, thalamus, cerebellum, and ventricles. A negative BOLD signal (deactivation) was mainly located in the anterior frontal lobe, basal ganglia, cingulated gyrus, and precuneus. The

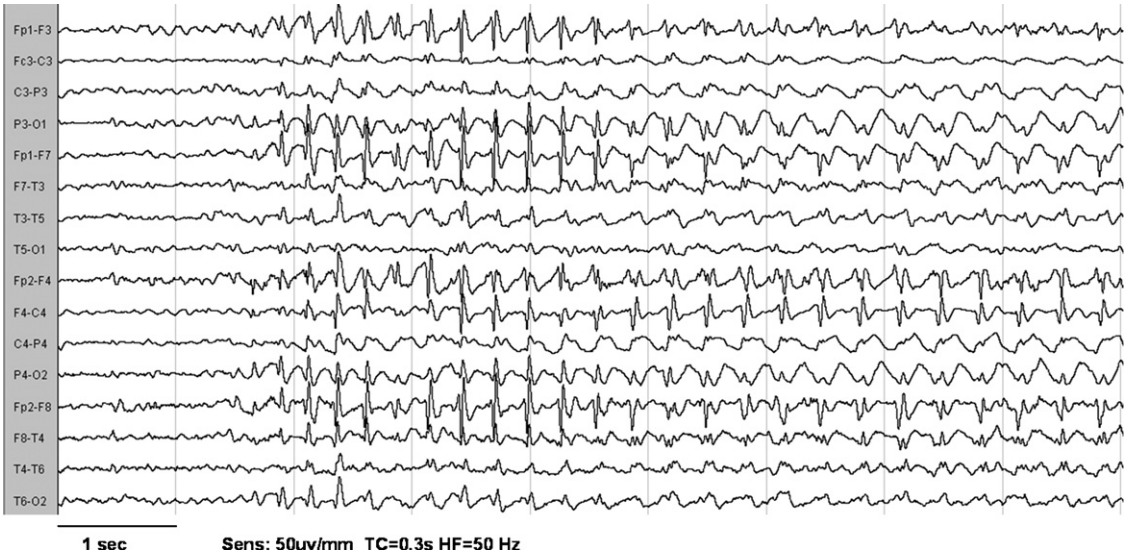

Figure 1 EEG recorded during scanning following artifact correction. Patient 5 showed 3—4 Hz GSWDs arising from normal background activity which are displayed as a bipolar montage.

regions of significant BOLD signal changes are shown in Table 2 and Figs. 2 and 3. In patients (nine sessions) with interictal GSWDs, activation was mainly located in the cortical areas (seven sessions) and next, most frequently, in the thalamus bilaterally (three sessions); two sessions did not show activation. Deactivation was observed in cortical regions (eight sessions) and the caudate nucleus (seven sessions). In patients (eight sessions) with ictal GSWDs, activation was located both in the thalamus (six sessions) and cortical regions (six sessions), and deactivation was noted in cortical regions (eight sessions) and the caudate nucleus (seven sessions).

The individual maximum t value was larger for ictal GSWDs (activation: 10.15 ± 3.09; deactivation: -16.34 ± 6.08) than for interictal GSWDs (activation: 5.20 ± 1.10; deactivation: $-4.85.3 \pm 1.10$). The individual total volume of the BOLD signal was larger for ictal GSWDs (activation: $63.14 \pm 21.56\,cm^3$; deactivation: $682.82 \pm 309.35\,cm^3$) than for interictal GSWDs (activation: $8.13 \pm 3.89\,cm^3$; deactivation: $37.63 \pm 20.92\,cm^3$). A significant difference in the maximum t value and the total volume between the BOLD response to ictal and interictal GSWDs was found by performing non-parametric comparison ($P < 0.001$). This suggests a BOLD response with a higher amplitude and more widespread extent at the time of the ictal GSWDs as compared to the time of interictal events.

Group analysis

In the interictal GSWD group, no activation in the suprathreshold clusters was found. The positive signal changes in some subjects and the negative ones in others in the same region may lead to a loss of this effect at the group level. The largest region of deactivation was located in the frontal lobe ($3.24\,cm^3$), and the largest cluster was located in the middle frontal gyrus ($1.66\,cm^3$) with the maximum t value (-22.04). There were several large clusters observed in the occipital, parietal, temporal, and limbic lobes and caudate nucleus.

In the ictal GSWD group, the analysis indicated that a group effect of the bilateral thalamic signal increased. The largest cluster of activation was located in the right thalamus and lateral ventricle ($1.47\,cm^3$), with the maximum t value in the thalamus (21.56). The largest cluster of deactivation was found in the medial frontal gyrus ($5.53\,cm^3$), and the maximum t value of deactivation was found in the cingulate gyrus (-54.20). Obvious deactivation was detected in the whole basilar ganglia including the caudate nucleus, claustrum, and lentiform nucleus. Large regions of deactivation were observed in the limbic lobes including the cingulate gyrus bilaterally and posterior cingulate, and the occipital lobe including the precuneus.

Group analysis also showed that BOLD signal changes with a higher amplitude and more widespread extent in the ictal GSWD group. The regions of significant BOLD changes were revealed with coordinates of volumes and their respective t values (Table 3). The group effect of BOLD changes in response to GSWDs is shown in Fig. 4.

Discussion

The patterns of BOLD changes in response to GSWDs in patients with absence epilepsy had the following features: (1) activation and deactivation were generally located bilaterally and symmetrically; (2) activation was located in the thalamus and cortical regions, and the maximum activation area was predominantly in the thalamus when associated with ictal GSWDs and mainly in the cortical regions when associated with interictal GSWDs; deactivation was widespread and distributed in the cortex and basal ganglia; and (3) ictal GSWDs were associated with a more widespread extent and a higher amplitude of BOLD signal changes than were interictal GSWDs.

Our study showed that thalamic activation is associated with ictal GSWD bursts in patients with CAE, which is consistent with previous EEG—fMRI studies on GSWDs (Salek-

Table 2 Number and duration of discharges and regions of significant BOLD signal change for all sessions during which interictal and ictal GSWDs occurred.

Epileptic activity	ID no	No. of GSWDs	Duration of GSWDs. Median (range) (s)	Regions of significant fMRI signal change										
				Thalamus	Frontal	Parietal	Temporal	Occipital	Precuneus	Posterior cingulate	Caudate nucleus	Brainstem	Cerebellum	Lateral ventricles
Interictal	1	12	1(0.7—3.2)	—	↑B;↓B m	↑B m	—	↓B	—	—	—	—	—	—
	3a	4	1.6(1.0—1.8)	—	↑B m; ↓B m	↓B	↓B	↓B	↓B	—	↓B	—	—	—
	3b	12	1.6(0.9—3.0)	↑B	↑B m; ↓B	↑B	↑B;↓B	↑B	↓B	—	↓L m	—	↑B	↑B
	5a	6	1.1(0.5—1.9)	—	↑B m; ↓B m	↓ R	↓ B	↑R; ↓B	↓ R	—	↓B	B↓	L↓	R ↑
	5b	8	1.2(0.9—2.2)	—	↑B;↓R	↑B m; ↓B	—	↓B	—	↓B m	↓B	—	—	—
	6	3	1.2(0.6—1.8)	—	—	—	—	—	—	—	—	—	—	—
	8	4	1.0(0.7—1.3)	—	↓B	—	↓B	—	—	↓B	↓B	—	—	—
	10a	14	1.7(1.0—3.8)	↑ B	↑B m; ↓B	↑ B	↑ B	—	↓B m	↓B	↓B	—	↑B	↑B
	10b	8	1.5(1.0—2.1)	—	↓B	↓B	—	↓B	—	↓B	↓B m	—	—	—
	12	3	1.0(0.8—1.9)	↑ B	↑B	↑B m	↓B m	—	—	—	—	—	—	—
Ictal	2	1	23.0(23.0—23.0)	↑B m	↑B; ↓B	↓B	↓B m	↓B	↓B	↓B	—	—	—	↑B
	4	2	9.0(8.0—10.0)	↑B m	↓B	↓B	↓B	↓B	↓B	↓B	↓B	—	—	↑B
	5c	2	17.8(15.0—20.5)	—	↓B m	↓B	↓B	↓B	↓B	↓B	↓B	—	—	—
	5d	5	11.8(9.3—25)	↑B m	↑B;↓B m	↓B	↓B	↓B	↓B	↓B	↓ B	↓ B	—	↑B
	7a	1	28.0(28.0—28.0)	↑B m	↑B;↓B	↑B	—	↓ B;↑B	↓B	↓B	↓ B	↓ B	↑B;↓ B	—
	7b	1	19.5(19.5—19.5)	↑B m	↑B;↓ B m	↓B	—	↓B	↓B	↓B	↓ B	↓B	↑B; ↓B	—
	11	3	30.0(26.0—35.0)	↑B	↓B	↓B	↓B	↓B	↓B	↓B	↓B	↓B	↑B m; B↓	↑B
	13	11	17.0(10.2—27.4)	—	↑B;↓B m	↓B	↓B	↑B m; ↓B	↓ B	↓ B	↓B	↓B	↓B	—

ID no.: identification number, corresponds to that in Table 1; (a), (b), (c) and (d) are given for patients studied during four sessions; ↑: increase; ↓: decrease; B: bilateral; L: left; R: right; m: maximum *t*-value.

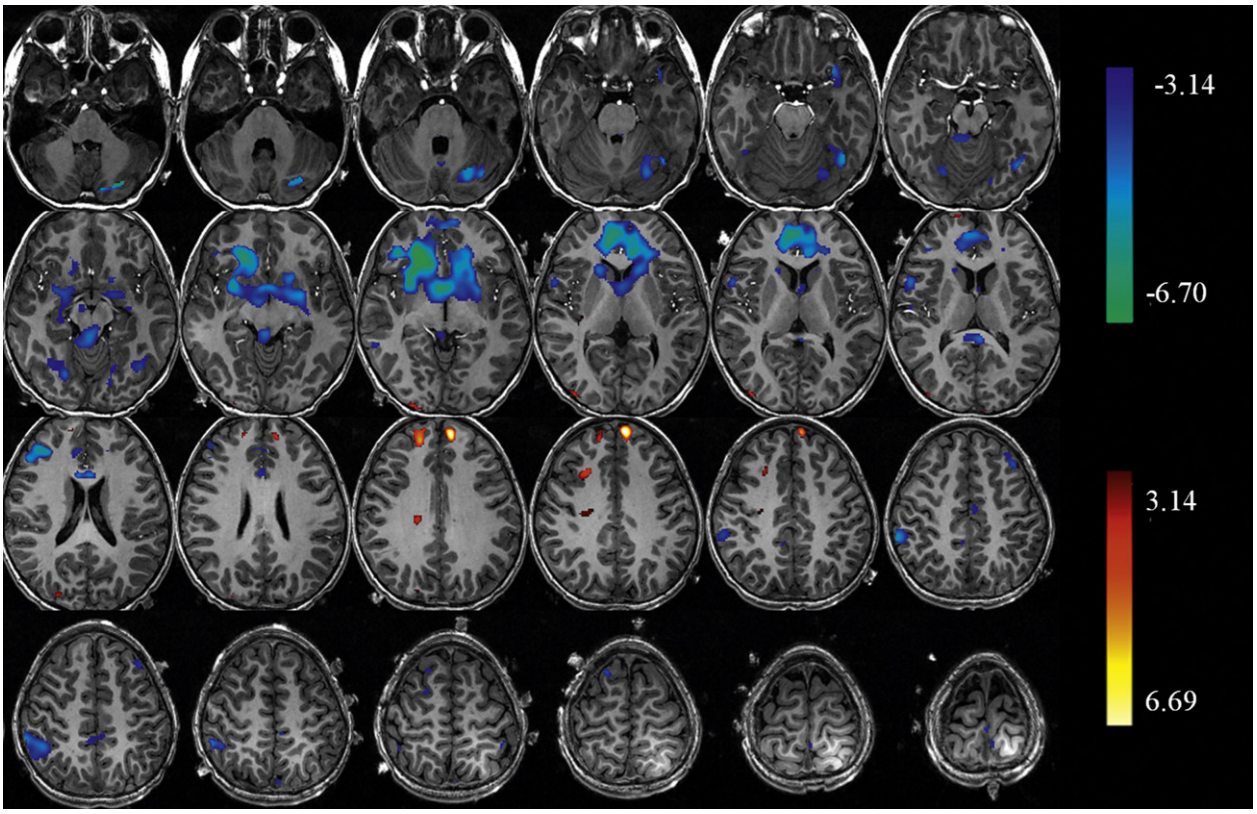

Figure 2 BOLD signal changes in response to interictal GSWDs of Patient 5. Activation in the bilateral superior frontal gyrus (the highest *t* value and maximum volumes), right middle frontal gyrus, and right occipital lobe; deactivation in the bilateral middle frontal gyrus (the highest *t* value and maximum volumes), middle temporal gyrus and caudate nucleus, left anterior cingulate, and left cerebellum.

Haddadi et al., 2003; Moeller et al., 2008a). Although the relationship between the thalamus and cortex in the mechanism of GSWD paradoxical discharges has still not yet been defined, thalamic activation in our study was consistent with its known role of involvement in generating GSWDs. Our study found that in most patients with interictal GSWDs, the maximum activation was predominantly in the cortex. This finding is not consistent with those of most previous studies in which the maximum activation was in the thalamus (Aghakhani et al., 2004; Gotman et al., 2005; Laufs et al., 2006). On the other hand, the BOLD signal in response to ictal GSWDs showed maximum thalamic activation. Interestingly, one patient (patient 5) whose BOLD changes in response to both ictal and interictal GSWDs were obtained in the two successive EEG—fMRI scanning sessions also showed this feature (Figs. 2 and 3). Therefore, we propose that the detection of thalamic activation in individual cases may in part be related to the duration of GSWD epochs recorded. GSWDs with a longer duration may be prone to present stronger thalamic activation. This finding is consistent with a previous study which showed that thalamic activation represents subcortical activity necessary for the maintenance of GSWDs (Avoli et al., 2001). Of course, thalamic activation associated with interictal GSWD burst may be detected because of the higher sensitivity of fMRI or other methods of fMRI analysis (Laufs et al., 2006).

The spatial pattern of deactivation during interictal and ictal GSWDs was strikingly similar in the frontal cortical areas, parietal areas, and precuneus, which is in accordance with the findings of previous studies (Salek-Haddadi et al., 2003; Aghakhani et al., 2004; Labate et al., 2005; Hamandi et al., 2006; Laufs et al., 2006; Moeller et al., 2008a) and has been interpreted in the context of the ''default mode network'' (Raichle and Mintun, 2006; Laufs, 2008). According to this hypothesis, the parietal cortex, precuneus, and frontal cortical areas are active at rest and maintain consciousness in people while they are awake. The abnormal thalamocortical synchronization during GSWDs disrupts the thalamocortical and corticocortical connectivity among cortical regions that constitute the ''default mode network.'' The abnormal thalamocortical synchronization reduces the level of cortical activity in these regions and may represent a hemodynamic correlate of impaired consciousness during absence seizures (Gotman et al., 2005; Hamandi et al., 2006; Laufs et al., 2006). However, the loss of consciousness is not always complete during absence seizures (Gloor, 1986) and may correlate with the duration of the absences (Van Luijtelaar et al., 1991). In our study, negative BOLD responses with a higher amplitude and more widespread extent were observed with a longer duration of GSWDs (ictal events). We suggest that the ictal epileptic discharges (a long duration of GSWDs) resulting from abnormal thalamocortical synchronization cause a severe disturbance or suspension of the default mode network, manifesting widespread cortical deactivation and clinical loss of consciousness. Meanwhile, interictal epilep-

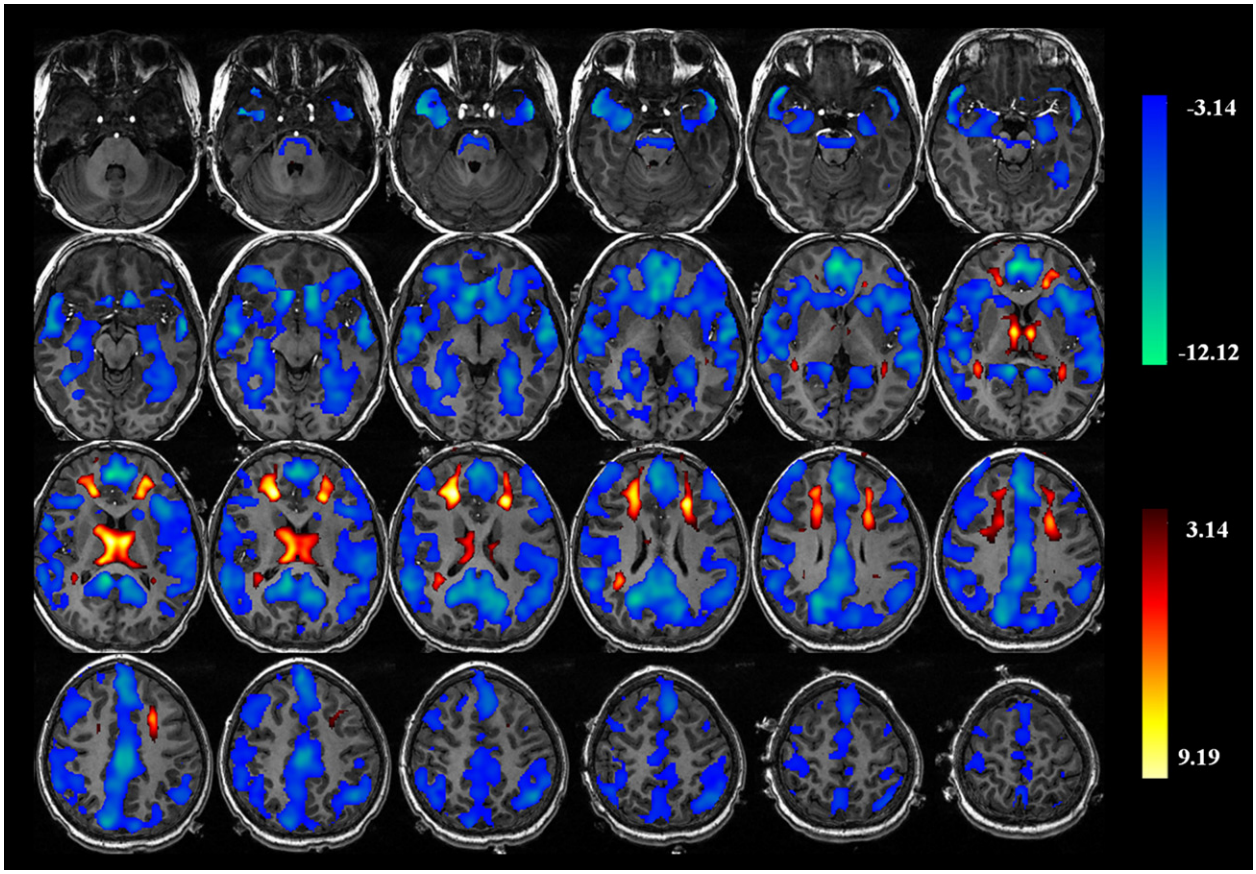

Figure 3 BOLD signal changes in response to ictal GSWDs of Patient 5. Activation in the thalamus bilaterally (the highest *t* value), superior and middle frontal gyrus bilaterally (maximum volumes), occipital cortex bilaterally, and posterior cingulate; deactivation in the caudate nucleus bilaterally (the highest *t* value), uncus bilaterally (maximum volumes), middle frontal gyrus and posterior cingulate bilaterally, and brainstem.

tic discharges (a short duration of GSWDs) only cause a partial suspension of the default state of the brain, and impairment of consciousness cannot been observed clinically.

So far, reports on BOLD changes in response to GSWDs in the basal ganglia have been less consistent in humans, and the deactivation of the caudate nucleus has seldom been reported in group analysis in patients with different sub-

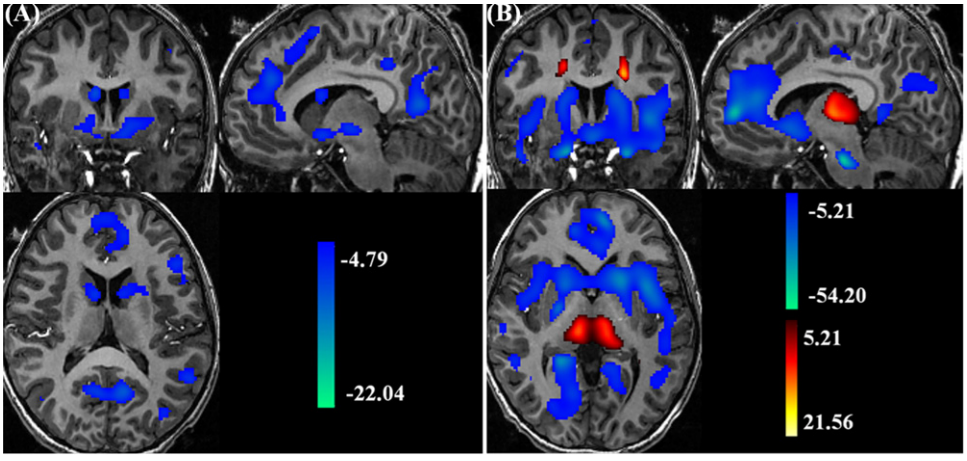

Figure 4 The second level group analysis for the patients with GSWDs. (A) BOLD signal in response to interictal GSWDs: deactivation mainly distributed in the middle frontal gyrus bilaterally and diffusely in the precuneus, claustrum, cingulate gyrus, posterior cingulate nucleus, and parietal, occipital, and temporal lobes. (B) BOLD signal in response to ictal GSWDs: activation in the thalamus and lateral ventricle, and deactivation in the frontal areas, parietal areas, precuneus, and in the basal ganglia bilaterally.

Table 3 Significant BOLD signals in response to GSWDs located by brain region.

Interictal GSWDs				Ictal GSWDs			
Region	Side	*t*-Value	Volume (cm^3)	Region	Side	*t*-Value	Volume (cm^3)
Activation							
—	—	—	—	Thalamus	R	21.56	1.47[a]
				Thalamus	L	7.46	0.15[a]
				Lateral ventricle	R	12.58	1.47[b]
				Frontal lobe, white matter	L	8.91	0.14
				Parietal lobe, white matter	L	16.05	0.18
				Midbrain	L	7.82	0.15[b]
Deactivation							
Frontal lobe							
Middle frontal gyrus	R	−22.04	1.66	Medial frontal gyrus	R	−25.31	5.53
Inferior frontal gyrus	L	−8.85	1.02	Inferior frontal gyrus	L	−32.95	0.78
Parietal lobe							
Inferior parietal lobule	L	−8.42	0.72	Postcentral gyrus	L	−15.72	0.13
Temporal lobe							
Superior temporal gyrus	L	−5.38	0.10	Middle temporal gyrus	R	−39.87	3.56[a]
				Middle temporal gyrus	R	−14.15	1.54
Occipital lobe							
Superior occipital gyrus	R	−7.77	1.49	Middle occipital gyrus	L	−33.01	0.91
Precuneus	R	−9.54	1.04	Precuneus	R	−36.61	3.56[b]
				Precuneus	R	−11.44	2.45[a]
Limbic lobe							
Posterior cingulate	L	−5.82	0.26	Cingulate gyrus	L	−54.20	2.45[b]
Cingulate gyrus	L	−6.54	0.37	Cingulate gyrus	R	−11.11	2.45[b]
				Posterior cingulate	R	−36.84	3.20
Basilar ganglia							
Caudate	R	−6.84	0.20	Caudate nucleus	R	−43.57	0.08
				Lentiform nucleus	L	−15.57	0.55
				Claustrum	R	−15.45	0.34

The same volume with 'a' and 'b' refers to two consecutive regions sharing the same cluster.

types of IGE (Hamandi et al., 2006; Moeller et al., 2008a). In our study, the BOLD signal decreased not only in the head of the caudate nucleus but also in the claustrum and lentiform nucleus during GSWDs paroxysms. Animal studies on genetic absence epilepsy rats from Strasbourg (GAERS) showed that the discharges recorded in the caudate nucleus occurred a few seconds after the discharges initiated in the thalamus or cortex (Danober et al., 1998); they also demonstrated that the basal ganglia circuits acted as a remote control system for absence seizure (Deransart and Depaulis, 2002). However, the role of basal ganglia deactivation in the pathophysiology of GSWDs in patients remains to be determined (Slaght et al., 2004). Although the mechanisms of propagation of epileptic discharges in the nuclei of the basal ganglia remain unknown, we propose that the BOLD changes in the basal ganglia may be a consequence of activity at the thalamocortical level, forming a basal ganglia—thalamocortical loop (Moeller et al., 2008a,b).

In conclusion, both interictal and ictal GSWDs in patients with CAE are associated with BOLD signal changes in the basal ganglia—thalamocortical network, which provides further evidence for basal ganglia—thalamocortical circuit involvement in the generation of GSWDs. Ictal GSWDs showing predominant thalamic activation and widespread cortical deactivation might cause complete suspension of the brain's default state and manifest clinically as abrupt loss of consciousness (absence seizures).

Disclosure

The study was performed according to the standards set by the Declaration of Helsinki. The study was approved by the Ethics Committee of West China Hospital.

Conflicts of interest

The authors reported no conflicts of interest.

Acknowledgements

This study was supported by National Natural Science Foundation of China (Grant Nos. 30625024 and 30728017), the National Basic Research Program (973 Program No: 2007CB512305), and the National High Technology Program

of China (863 Program No: 2008AA02Z408). The authors thank Dr. Rongbi Cao, Dr. Yi Jiang, and Dr. Guanggu Yuan (Department of neurology, West China Hospital of Sichuan University, China) for referring patients. This study was also sponsored by the program of International Cooperation and Exchange of National natural science foundation of China (No. 30811120424).

References

Aghakhani, Y., Bagshaw, A.P., Bénar, C.G., Hawco, C., Andermann, F., Dubeau, F., Gotman, J., 2004. fMRI activation during spike and wave discharges in idiopathic generalized epilepsy. Brain 127, 1127—1144.

Avoli, M., Rogawski, M.A., Avanzini, G., 2001. Generalized epileptic disorders: an update. Epilepsia 42, 445—457.

Commission on Classification Terminology of the International League Against Epilepsy, 1981. Proposal for revised clinical and electroencephalographic classification of epileptic seizures. Epilepsia 22, 489—501.

Danober, L., Deransart, C., Depaulis, A., Vergnes, M., Marescaux, C., 1998. Pathophysiological mechanisms of genetic absence epilepsy in the rat. Prog. Neurobiol. 55, 27—57.

Deransart, C., Depaulis, A., 2002. The control of seizures by the basal ganglia? A review of experimental data. Epileptic Disord. 4, S61—S72.

Engel Jr., J., International League Against Epilepsy (ILAE), 2001. A proposed diagnostic scheme for people with epileptic seizures and with epilepsy: report of the ILAE Task Force on Classification and Terminology. Epilepsia 42, 796—803.

Friston, K.J., Jezzard, P., Turner, R., 1994. Analysis of functional MRI time-series. Hum. Brain Mapp. 1, 153—171.

Friston, K.J., Holmes, A.P., Poline, J.B., Grasby, P.J., Williams, S.C., Frackowiak, R.S., Turner, R., 1995. Analysis of fMRI time-series revisited. Neuroimage 2, 45—53.

Friston, K.J., Fletcher, P., Josephs, O., Holmes, A., Rugg, M.D., Turner, R., 1998. Event-related fMRI: characterizing differential responses. Neuroimage 7, 30—40.

Garreffa, G., Carnì, M., Gualniera, G., Ricci, G.B., Bozzao, L., De Carli, D., Morasso, P., Pantano, P., Colonnese, C., Roma, V., Maraviglia, B., 2003. Real-time MR artifacts filtering during continuous EEG/fMRI acquisition. Magn. Reson. Imaging 21, 1175—1189.

Gloor, P., 1986. Consciousness as a neurological concept in epileptology: a critical review. Epilepsia 27, 14—26.

Gotman, J., Grova, C., Bagshaw, A., Kobayashi, E., Aghakhani, Y., Dubeau, F., 2005. Generalized epileptic discharges show thalamocortical activation and suspension of the default state of the brain. PNAS 102, 15236—15240.

Gotman, J., 2008. Epileptic networks studied with EEG—fMRI. Epilepsia 49 (Suppl. 3), 42—51.

Hamandi, K., Salek-Haddadi, A., Laufs, H., Liston, A., Friston, K., Fish, D.R., Duncan, J.S., Lemieux, L., 2006. EEG—fMRI of idiopathic and secondarily generalized epilepsies. Neuroimage 31, 1700—1710.

Hanneke, M., van Luijtelaar, G., da Silva, F.L., Coenen, A., 2005. Evolving concepts on the pathophysiology of absence seizures: the cortical focus theory. Arch. Neurol. 62, 371—376.

Labate, A., Briellmann, R.S., Abbott, D.F., Waites, A.B., Jackson, G.D., 2005. Typical childhood absence seizures are associated with thalamic activation. Epileptic Disord. 7, 373—377.

Laufs, H., Lengler, U., Hamandi, K., Kleinschmidt, A., Krakow, K., 2006. Linking generalized spike-and-wave discharges and resting state brain activity by using EEG/fMRI in a patient with absence seizures. Epilepsia 47, 444—448.

Laufs, H., Duncan, J., 2007. Electroencephalography/functionalMRI in human epilepsy: what it currently can and cannot do. Curr. Opin. Neurol. 20, 417—423.

Laufs, H., 2008. Endogenous brain oscillations and related networks detected by surface EEG-combined fMRI. Hum. Brain Mapp. 29, 762—769.

Moeller, F., Siebner, H.R., Wolff, S., Muhle, H., Granert, O., Jansen, O., Stephani, U., Siniatchkin, M., 2008a. Simultaneous EEG—fMRI in drug-naive children with newly diagnosed absence epilepsy. Epilepsia 49, 1510—1519.

Moeller, F., Siebner, H.R., Wolff, S., Muhle, H., Boor, R., Granert, O., Jansen, O., Stephani, U., Siniatchkin, M., 2008b. Changes in activity of striato-thalamo-cortical network precede generalized spike wave discharges. Neuroimage 39, 1839—1849.

Raichle, M.E., Mintun, M.A., 2006. Brain work and brain imaging. Annu. Rev. Neurosci. 29, 449—476.

Salek-Haddadi, A., Lemieux, L., Merschhemke, M., Friston, K.J., Duncan, J.S., Fish, D.R., 2003. Functional magnetic resonance imaging of human absence seizures. Ann. Neurol. 53, 663—667.

Slaght, S.J., Paz, T., Chavez, M., Deniau, J.M., Mahon, S., Charpier, S., 2004. On the activity of the corticostriatal networks during spike-and-wave discharges in a genetic model of absence epilepsy. J. Neurosci. 24, 6816—6825.

Stern, J.M., 2006. Simultaneous electroencephalography and functional magnetic resonance imaging applied to epilepsy. Epilepsy Behav. 8, 683—692.

Tyvaert, L., Hawco, C., Kobayashi, E., LeVan, P., Dubeau, F., Gotman, J., 2008. Different structures involved during ictal and interictal epileptic activity in malformations of cortical development: an EEG—fMRI study. Brain 131, 2042—2060.

Van Luijtelaar, E.L., de Bruijn, S.F., Declerck, A.C., Renier, W.O., Vossen, J.M., Coenen, A.M., 1991. Disturbances in time estimation during absence seizures in children. Epilepsy Res. 9, 148—153.